Effects of Heat Treatment and Surface Finish on the Crevice Corrosion Resistance of Martensitic Stainless Steel

Dr. Haider M. Mohammad
Department of Material Engineering
University of Basrah
College of Engineering
drhaidermaath@gmail.com

Fatima Sameer Ahmed
Department of Mechanical Engineering
University of Basrah
College of Engineering
fatimashabaan57@gmail.com

Abstract- **The present study aims to investigate the influence of heat treatment and surface finish on the behavior of crevice corrosion resistance of AISI 410 and 416 martensitic stainless steels thus, to quantify the conditions at which crevice corrosion minimize as possible. The experimental work carried out during this study involves material selection, chemical composition tests, specimens preparation before heat treatments, austenitizing at temperature range (925-1010˚C) and for holding time periods of (30, 45 and 90 min), air and oil quenching followed by tempering at heating range of (205-605˚C) and for 45 min, micro hardness tests, specimens grinding, surface roughness measurements, crevice corrosion tests, crevice evaluation and microstructure tests. Theoretically, empirical equations for crevice maximum depth under the effect of surface roughness and hardness for both AISI 410 and 416 steels were determined. While for microstructure analysis, carbides average area was determined by using the ImageJ analysis program and a mathematical model was also predicted. Results showed that, as hardness and surface roughness increase crevice corrosion resistance decreases. Therefore, material treated by annealing can minimize crevice corrosion rates more than that treated with hardening.**

***Index Terms*—Austenitizing, Crevice, Corrosion, Carbides, Hardness, Roughness, Tempering.**

I. INTRODUCTION

In most engineering applications requiring high durability, corrosion resistance is one of the most important requirements that must be provided. Such importance attributed to three main factors; economics, safety and conservation. Each factor control corrosion considerably. One of the most significant localized corrosion is crevice corrosion, which is often occurs in occluded locations.

Most of previous studies were concerned with studying the behavior of corrosion for carbon and low alloy steels. However, the rapidly increasing number of applications and the need for superior properties in specific applications led to several attempts to widen research fields in the performance improvement of stainless steels. For stainless steels, martensitic stainless steels are the smallest but the most scalable category due to their hardenability by heat treatments. For martensitic group, there is a wide range of applications which often exposed to the risks of localized corrosion such as; steam generators, boilers, bolts, turbine blades, and others [1].

Screws and fasteners are prevalent sources of crevice corrosion attacks. Replacing rusty bolts with new one is more costly than using expensive corrosion resistance fasteners from the beginning. Therefore, there was a need to use an appropriate stainless steel metal and improve its quality by studying the effects of heat treatments and surface finish on its crevice corrosion resistance.

For martensitic stainless steels, heat treatments are the same for low alloy steels or plain carbon steels in which maximum hardness depends mainly on the carbon content. The only difference is that, for stainless steels the high content of alloying elements causes the structure transformations to be more sluggish [2].Heat treatments for ferrous metals comprise five principle processes:

- Hardening
- Case hardening
- Annealing
- Normalizing
- Tempering

Different results can be obtained by each process. All these processes involve three important stages that must be given the same degree of concern: heating, soaking (holding at the heating temperature for period of time) and cooling. Cooling rate is definite by several factors like mass and quenching media, and its considered as the controlling factor in which both properties and microstructure depend on [3].

On other side, surface topography is one of the most physical features of surfaces that has a significant influence on their technical properties. In general term topography defined as the distribution of elevations over a surface and the term can be specified by three characteristics:

- Lay: the direction of surface pattern.
- Surface roughness: the fine spaced irregularities produced by machining on the surface.
- Waviness: irregularities that more broadly spaced and produced as a result of vibrations during machining.

At engineering field, surface roughness and surface finish take the same meaning. It was considered that such roughness is attributed to the different shear orientation spreading across the surface during manufacturing. Particularly, surface roughness as a result of plastic deformation over free surfaces depends on several determinants such as surface initial situation, grain size, deformation and isotropy. Surface roughness described by number of parameters and the most common use one is the average roughness parameter (Ra) which represents the average of elevations (asperities) and bottoms over the whole measured area. Surface finish has a significant effect on metals with passive films, as in the case of stainless steel due to the existence of chromium content in the oxide film [4].

Many attempts have been carried out by researchers in order to cover corrosion field within different aspects. However, studies related with crevice corrosion were limited. Many researchers focused their efforts in the direction of studying the effects of heat treatments on pitting corrosion behavior of stainless steel, while limited studies were concerned with studying there effects on crevice corrosion.

For heat treatment effects, **J. E. Truman (1976)**studied the effects of tempering process for a range of temperatures and time periods on the corrosion resistance of several grades of 13 % Cr martensitic stainless steel by using the method of different in weight for corrosion rate determination. Results showed that as hardness increased by tempering, corrosion rates were also increased and attributed such behavior to the precipitations of chromium carbides [5].

As well, **R. Godec and V. Dolecek (1994)** investigated the effects of carbides alterations in martensitic stainless steels as a result of heat treatments under the effects of three aggressive solutions with different chloride concentrations. The investigations resulted that as tempering temperature decreases, the carbide precipitation increases and therefore for samples with higher carbide concentrations the pitting corrosion rates increase by increasing the chloride concentrations more than that with lower carbides contents [6].

For surface roughness effects, according to **G. T. Burstein (1995, 2001),** the pitting corrosion rates decrease with increasing surface smoothness, and that attributed to the reducing of locations number that are capable of being motivated during corrosion reactions for smooth surfaces than that for rougher one **[7]-[8]**.

T. Hong and M. Nagumo (1997), found the same results as **Burstein** and attributed their results to the change in the determined value of E_m (the potential at which the pits begin to propagate on the surface) that increases with increasing the number of abrasive papers **[9]**.

While **W. Li and D.Y. Li (2006)**found that for rough surfaces, electrons at the peaks sites were more capable to escape than those in the bottoms (valleys), therefore peaks were susceptible to corrosion more favorably. Thus for corrosion at rough surfaces, as the electron energy of escaping from peaks increases as more of corrosion cells will be formed**[10]**.

II. MATERIALS

To select the adequate martensitic grade, important determinants must take into account:

- Corrosion and heat resistance
- Mechanical properties
- Fabrication operations
- Total cost

AISI 410 and 416 grades (1.4004 and 1.4005 according to EN numeric designation) are selected for their excellent hardenability through heat treating, moderate corrosion resistance in several chemical environments and for their good strength. In general, AISI 410 characterized by good corrosion resistance in mild and domestic atmosphere combine with excellent toughness in the hardened and tempered conditions. While, 416 characterized by excellent machinability coupled with acceptable strength in the hardened and tempered conditions [2].

III. EXPERIMENTAL WORK

A. Chemical Composition Test

The chemical compositions for both alloys were analyzed by using optical emission spectrometer analyzer device to confirm the constituents of elements. The results for both alloys can be shown in Table below. The results were compared with the standard results in the ASM metal handbook [2].

Table I The chemical composition of AISI 410 and 416 martensitic stainless steel in wt. %

Element	410 Chemical Composition %	410 ASM Results % [2]	416 Chemical Composition %	416 ASM Results % [2]
C	0.13	0.09-0.15	0.14	0.09-0.15
Mn	0.8	0-1.00	1.46	0-1.5
Si	0.4	0-1.00	0.32	0-1.00
S	< 0.027	0-0.03	0.28	0.15-0.35
Cr	12.71	11.5-13.5	13.35	12.0-14.0
Ph	< 0.03	0-0.04	< 0.03	0-0.06

As shown in Table (I), the chemical composition of AISI 410 steel contains 12.71% Chromium, 0.4% Silicon and 0.8% Manganese. Thus, such alloy can characterize by high hardenability with fairly good strength and corrosion resistance due to the high content of chromium compared with that of manganese. While the chemical composition for AISI 416 contains 13.35 % Chromium, 0.32 % silicon and 1.46 % manganese, which is higher than that for 410 steel. Thus, 416 steel can be characterized by its reasonable strength but with excellent machinability and hardenability. On other hand, the sulfur content for 410 steel is 0.027 %, while for 416 steel is 0.28 %. Therefore, 416 steel can reveal much lower corrosion resistance than that for 410 steel. Both alloys tends to form high carbides precipitations due to the high concentrations of Cr and Mn which regarded as strong carbide formers, compared to the Nickel and silicon that work as strong graphitizes (split up the carbides).

B. Specimens Machining and Preparation

Cold finished round bars of 410 and 416 steels were machined to 120 specimens (60 for each stainless steel grade) with the desired dimensions before receiving from the metal producing company in USA. AISI 410 specimens designed dimensions were:

- Diameter: 25.4 mm (1 inch)
- Thickness: 9.525 mm (0.375 inch)

While the designed dimensions for AISI 416 were:

- Diameter: 25.4 mm (1 inch)
- Thickness: 5.08 mm (0.2 inch)

After receiving, the specimens for both alloys were drilled in the center with 6.4 mm (0.251 inch) diameter (in order to accommodate the bolt for crevice corrosion test). Fig.1 shows a schematic design for the dimensions of specimens. After specimen machining, removing sharp edges which act as a stress riser locations and formed on the specimen surfaces during machining (cutting and drilling) was necessary before placing specimens into the heating furnace.

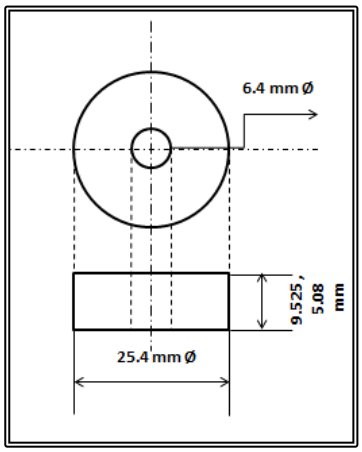

Fig. 1 Schematic design for the dimensions of stainless steel specimens.

C. Heat Treatments

Corresponding to ASM heat treating metals handbook [2], each of preheating, austenitizing, quenching and tempering treatments were carried out during this work for both alloys in order to examine their effects on the hardness.

C.1. Pretreatments

Preheating to a temperature below the transformation temperature is generally significant for the specimens to remove high residual stresses, high thermal gradients and to ensure that any effects of hardening processes carried previously on the specimens were removed [11].

For the present study, preheating was accomplished by using a rectangular furnace for temperatures above 955˚C, in addition to a cylindrical furnace for temperatures below 955˚C. During this study, pretreatments for both AISI 410 and 416 steels were carried out in two steps as following [2]:

1) First step: involved heating to 540˚C and continued for approximately 30 min until it was ensured that all parts of specimens reached the desired temperature.
2) Second step: involved heating to 790˚C and for the same period.

After heating stage, cooling was performed inside the furnace for 24 hr for both previous steps.

C.2. Austenitizing

For adjusting material properties and modifying their structures, austenitizing process was carried out according to the ASM handbook [2] for both alloys as following:

1) Both alloys were heated to the same heating temperature range (925-1010˚C).
2) The furnace reached the desired heating temperature after a sufficient period of time, and then held at that temperature for different periods.
3) AISI 410 specimens holding periods are 45 and 90 min, while AISI 416 specimens holding periods are 30, 45 and 90 min.
4) Air and oil quenching were used for AISI 410 specimens, while only oil quenching was used for 416 specimens.

C.3. Tempering

For reducing the retained austenite formed during austenitizing; relieving quenching stresses; ensuring dimensional stability and reducing the hardness values, a tempering process was carried out at a temperature range below the transformation temperature as following [2]:

1) For AISI 410 specimens, four tempering temperatures were utilized: (565 and 605˚C) maximum temperature limits, and (205 and 370℃) minimum temperature limits.
2) For AISI 416 specimens, four tempering temperatures were utilized: (565 and 605˚C) maximum temperature limits, and (230 and 370℃) minimum temperature limits.
3) Held at such temperatures for 45 min for both alloys.
4) Air cooling was used for both alloys.

D. Micro Hardness Tests

Corresponding to the ASM heat treating handbook [2], hardness measurements were performed by using the micro-indentation tester and all the results were converted from Vickers to Rockwell. Simple wet grinding processes were carried out on the specimen surface before each test. Hardness measurements were performed into three stages for both alloys as following:

1) Before hardening: hardness ranging between 1 and 16 HRC.
2) After hardening: hardness ranging between 37 and 45 HRC.
3) After tempering: hardness ranging between 25 and 31 HRC for specimens tempered with 565 and 605˚C, and hardness ranging between 35 and 45 HRC for specimens tempered with 205 and 370˚C.

E. Specimens Grinding

Since crevice corrosion initiate at the beginning on the surfaces, such corrosion type depends strongly on the surface features. Therefore, studying the effects of surface roughness on crevice corrosion was important during this work.

Different surface roughness was obtained by performing a mechanical wet grinding by using a metallographic lapping/polishing machine with abrasive aluminum oxide papers of different grit numbers P (60, 80, 100, 150, 220, 320, 400, 500, 600, 800, 1000, and 1200) arranged from the rougher to the smoother one.

F. Surface Roughness Measurements

Surface roughness tester used during this study to measure the different surface roughness obtained from grinding operations. After calibrating the device, each specimen was tested several times at many areas on both surfaces, and the average was determined. Ra (roughness factor) was calculated by the device according to the following equation:

$$Ra = \frac{1}{n}\sum_{i=1}^{n}|y_i| \quad (1)$$

Where, Ra represents the arithmetic average roughness (μm), n represents the number of peaks within sampling length, and yi represents the vertical distances from the mean line (μm).

Fig. 2 shows the surface roughness measurement device used during this study.

G. Crevice Corrosion Tests

Crevice corrosion test method was carried out according to the ASTM designation G 48-00 (method D-Critical

crevice temperature test) which is under the jurisdiction of ASTM Committee G01 on corrosion of metals [12].
Since surface conditions can significantly influence the crevice corrosion results, air passivation after grinding for more than 24 hr was important in order to minimize the effects of grinding on the surface passive layer.

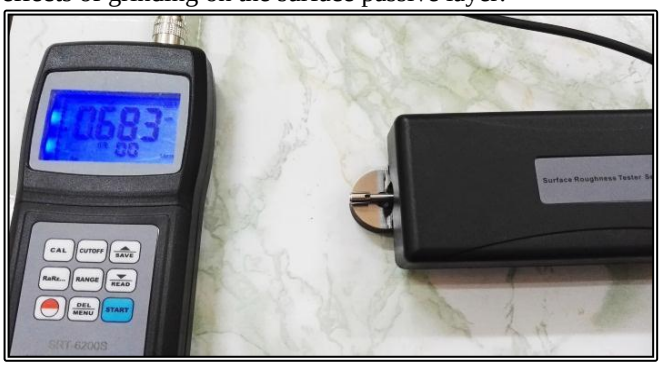

Fig. 2 The surface roughness measurement device

G.1. Crevice Formers

For crevice tests, 120 Teflon-fluorocarbon crevice washers (two for each specimen) were machined from Teflon round rod according to the standard [12] as following: each crevice washer was machined with outside diameter of 20 mm, thickness of 10 mm, and then drilled in the center with inside diameter of 6.4 mm. After that, 12 grooves were machined with the same depth on both surfaces of the washer by using a milling machine. Fig. 3shows a schematic design for the dimensions of TFE-fluorocarbon crevice washers.

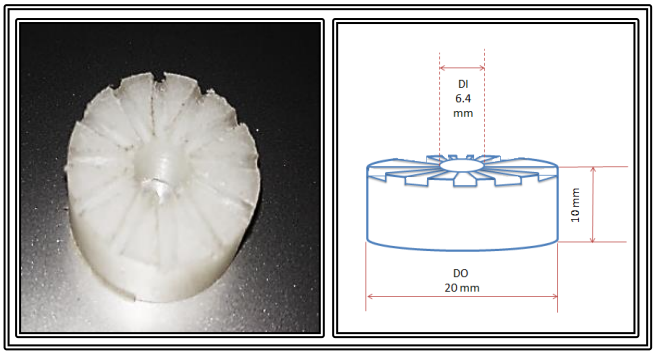

Fig. 3 Schematic design for the dimensions of TFE-fluorocarbon crevice washers

Threaded bolts of stainless steel with 50 mm length and 6 mm diameter, in addition to stainless steels flat washers and nuts were used for the purpose of joining the crevice washers with the specimens.

G.2. Test Solution Preparation

The ferric chloride solution was prepared by adding 16 ml of HCl acid concentrated with (36.5-38.0 %) to 600 ml of distilled water into a wide mouth flask of 1000 ml size. 68.72 g of $FeCl_3$ (ferric chloride) powder was balanced and added to the previous solution, and then mixed together. The resulting solution was $FeCl_3.6H_2O$ which contained about 1% HCl and 6% $FeCl_3$. Finally, the solution was filtered by filtering papers. Fig. 4 shows the prepared ferric chloride solution during filtering.

Fig. 4 The prepared ferric chloride solution ($FeCl_3.6H_2O$) during filtering

G.3. Crevice Corrosion Tests Method

The crevice formers (bolt, two nuts and two flat washers) were used to fasten the two crevice washers together with the specimen from both sides. Torque limiting nut driver was used to apply 0.28 Nm of torque so that connection can't be loosed during test according to the ASTM designation G 84-00 [12]. Although bolt, nuts and flat washers were made of stainless steels, but they can be corroded aggressively by ferric chloride solution and cause loosening of connection. Therefore, each of them were wrapped with a Teflon tape and covered with red oxide primer paint as illustrated in Fig. 5.

When the red primer paint was dried, the specimen was immersed inside 250 ml of ferric chloride solution (after reached the room temperature). All tests for both alloys were carried out at the same temperature (room temperature), for the same solution amount, and no more than one specimen was immersed inside the flask. Each specimen was immersed for 72 hr according to the standard test period in G 48 designation [12]. After the test period has elapsed, the specimen was removed from solution, rinsed with water and scrubbed with nylon brush under water to remove corrosion and solution products, then dipped into acetone and air dried.

Fig. 5 Protecting operations of bolt, nuts and flat washers against corrosion

H. Crevice Depth Examination and Evaluation

Crevice examination and evaluation were conducted according to the ASTM G 48-00 standard designation [12]. A visual examination of the corroded steels surfaces was carried out under the ordinary light to identify the existence of crevice corrosion on both specimen surfaces under the TFE-fluorocarbon washers, to ensure that crevice formers connection with specimen kept fix during the test period and to ensure crevices right locations on surfaces.

For more detailed examination, the measurements of crevices maximum depth were carried out by using a needle point micrometer that prepared by fixing a needle part on an electronic digital micrometer (0-25 mm/0.001 mm). The micrometer instrument was zeroed with the needle point before starting measuring, and then the needle point was attached to the crevice surface in order to measure the specimen thickness. After that, the needle was inserted in the crevice bottom and the specimen thickness was also measured. The difference between upper and bottom thickness represented the crevice depth. The test was performed for all 24 crevices on both specimen sides and the greatest crevice depth for each specimen was determined. Fig.6 shows crevice depth evaluation process.

Fig.6 Crevice depth evaluation process

I. Microstructure Tests

For studying the relation between hardness (resulted from heat treating) and the microstructure of both alloys, surface preparations before microstructure tests were carried out during this study according to the ASTM E3-01 standard guide for metallographic preparation [13].

Wet grinding operations were performed in two steps. The first step involved removing the disturbed surface layers produced during crevice test by using the lapping/Polishing machine and with P 180 (rough) abrasive papers. The second step involve removing the deformations from the first grinding step by using P 220, 400, 800 and 1200 abrasive papers sequentially from the rougher to the smoother for each specimen.

After grinding, polishing was performed in order to obtain surfaces with almost no scratches. Polishing clothes with diamond pastes of different small grain sizes (28, 20, 10, 3.5, 1 and 0.5 µm) were used sequentially from the larger grain size to the smaller.

The least surface preparation operation is represented by the etching process. An etching process was carried out to reveal the structural phases and inclusions of specimens that were difficult to be noticed before. This chemical removing was performed by the use of metallographic etchant prepared according to E 407 standard [14] by adding 5ml of HCl acid to 100 ml of ethanol, then 1 g of picric acid was balanced and added to the previous. After etchant preparing, the specimen surface was immersed for 2 min, removed, rinsed with distilled water and let to dry.

A metallurgical microscope with moderate-magnification lenses of 50× connected with a computer device was used in order to obtain photographic representation for the structural information of the specimens.

IV.THEORETICAL WORK

A. Regression for Crevice Maximum Depth

The relative crevice maximum depth equations vs. tempering hardness and surface roughness were found based on the experimental results obtained for both AISI 410 and 416 martensitic stainless steels.

For AISI 410 steels, an empirical equation with two parameters (A,B), 51 experimental point and 2 independent variables (tempering hardness and surface roughness factor) was found by using the LAB Fit program.

$$CMD = A \times HRC + B \times Ra^2 \quad (2)$$

Where, CMD represent the crevice maximum depth value, HRC represent the Rockwell hardness value after tempering while Ra represents the surface roughness factor. The equation constant values and the regression correlation coefficient are illustrated below.

- A = 0.55755883254E+01
- B = 0.99416709758E-04
- R = 0.971360E+00
- Radj² = 0.9423885E+00

For AISI 416 steels the same empirical equation (2), of AISI 410 steels but with 38 experimental points was found by using the LAB Fit program. The equation constant values and the regression correlation coefficient are illustrated below.

- A = 0.26942855858E+02
- B = 0.25229307276E-03
- R= 0.985696E+00
- Radj² = 0.9708075E+00

B. Image Analysis and Processing

For the purposes of microscopic images processing and analyzing, ImageJ program was used during this study. ImageJ can be defined as a common java image analysis and processing program that can be used for displaying, editing, analyzing, processing, saving and printing images of (32-bit, 16-bit or 8-bit).

During this work ImageJ was used for measuring the carbides amounts and areas in order to study the effects of carbides precipitations on stainless steel hardness values after tempering. The following steps represent the important procedures that were carried out by using the ImageJ:

- Image scale converting
- Contrast and brightness adjusting
- Threshold adjusting
- Noise removing (removing outliers)
- Filling holes
- Binary watershed
- ROI Manger Tool (Measurement)

C. Regression of Carbides Average Area

The relative carbides average area equation vs. tempering hardness was found based on the ImageJ results obtained for AISI 410 steel. An empirical equation with two parameters (A,B), 10 point and 1 independent variables (tempering hardness) was found by using the LAB Fit program.

$$CAA = A / HRC\hat{}2 + B \quad (3)$$

Where, CAA represents the carbides average area, while HRC represent the Rockwell hardness value after tempering. The equation constant values and the regression correlation coefficient are illustrated below.

- A = 0.4622729825E+02

- B = -0.89527014E-01
- R = 0.994590E+00
- Radj² = 0.9878601E+00

V. RESULTS AND DISCUSSION

A. Hardness Measurements

For the temperature range (925-1000˚C), hardness was approximately not changing too much (37-45 HRC). Then, when temperature increased, hardness decreased at the upper temperature limit (1010℃) and that was the same behavior remarked in the ASM metal handbook. According to the ASM handbook, the hardness decreasing at the upper temperature limit was attributed to the retained austenite formation due to the increasing of carbide dissolution with increasing austenitizing temperature [2].

For high tempering temperatures (565 and 605˚C), hardness reviled lower values than that for lower tempering temperatures (205-370℃) as shown in Fig. 7 and 8, and such behavior was attributed to the diffusing of carbon atoms that strained the iron lattice during quenching. The diffused carbon atoms reacted in a series of steps and formed Fe_3C thus, the properties of tempered steels depend on the size, shape and the location of distribution of the Fe_3C. As tempering temperature increase, the carbon atoms amount will be decrease by coalescence and therefore hardness will decrease. Sometimes tempering has only small effect on the hardness or even has no effect and hardness remains unchanged which attributed to the carbon atoms situation [11].

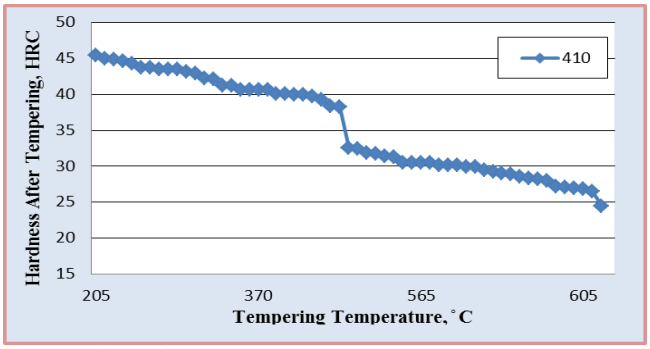

Fig. 7 Effects of tempering temperatures on the hardness for AISI 410

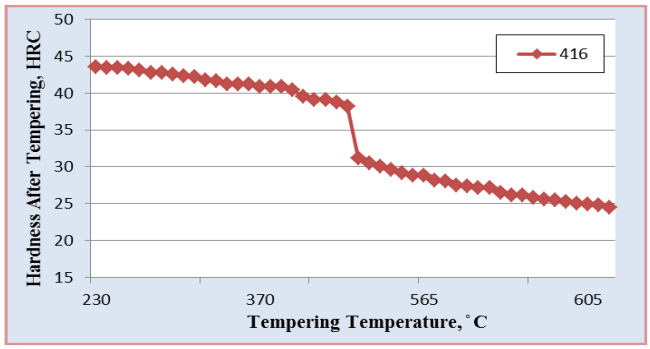

Fig. 8 Effects of tempering temperatures on the hardness for AISI 416

B. Crevice Depth Measurements

From experimental results and Equation (2), it can be observed that the surface roughness effects on the crevice maximum depth are higher than that for hardness, and as hardness and surface roughness increase, crevice maximum depth also increases. This behavior can be illustrated in Fig.9 and 10.

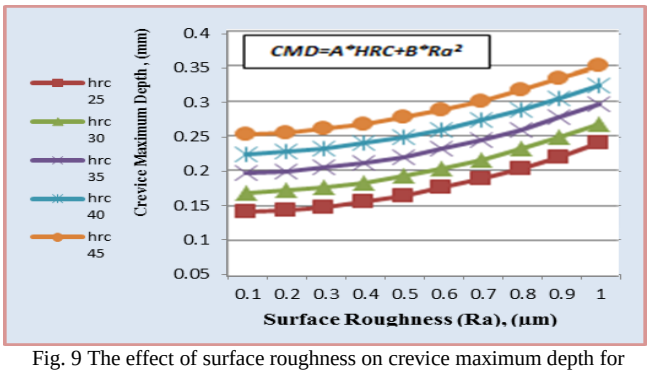

Fig. 9 The effect of surface roughness on crevice maximum depth for different harnesses for AISI 410 steel

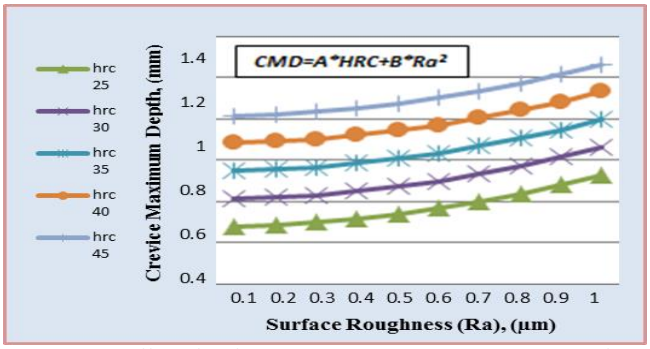

Fig. 10 The effect of surface roughness on crevice maximum depth for different harnesses for AISI 416 steel

The previous behaviors can be discussed as following:

B.1. Tempering Effects

Heating martensite (results by quenching from high temperatures) to the tempering temperatures (low temperature) and then air cooled, resulted with the formation of a structure that consist of α-iron and cementite particles (dispersed iron carbide Fe_3C), such brittle structure is known as tempered martensite. These two phases causes the corrosion reaction to be accelerated in rates depending on the amount of finally divided cementite. From that, the properties of tempered martensite are specified particularly by size, shape, amount and distribution of carbides.

At tempering temperature below 400˚C, cementite particles are small in size, large in amount and distributed in many areas in the structure which are the reasons after the high hardness values that caused high crevice corrosion reactions. While, for tempering temperatures above 400˚C, cementite particles coalesces and form large particles size with small amounts thus, making the structure more resistance of dissolution in acids and therefore lower hardness values will be resulted and causing lower corrosion rates [11]-[15].

In addition to the Fe_3C carbides, alloying carbides have certain effects on the tempered martensite properties as follows; the main purpose of adding alloying elements to the martensitic stainless steel is to improve the ability of forming martensite (hardenability). For martensitic stainless steels, the based alloying element in such steels is the chromium which represents a strong carbides former element. Carbide formers main objective is to retard the softening process by formation of carbides that precipitate on the grain boundaries [11].

In this study chromium high concentration for both AISI 410 and 416 was the reason after forming high chromium carbides, in addition to the cementite formed during tempering, both carbides increased the brittleness of

tempered martensite, subsequently increased the hardness and as result, accelerated the crevice corrosion reaction. Therefore, the reasons after increasing crevice corrosion by increasing hardness for both 410 and 416 types were referred to the presence of Fe_3C and chromium carbides in the tempered martensitic structure.

As well from crevice maximum depth results, AISI 416 steel revealed higher crevice corrosion depth than AISI 410 steel and this behavior can be attributed to the following; AISI 416 steel contains higher concentration of sulfur than AISI 410 steel, but the same concentrations of phosphorus as indicated in Table (I). Both phosphorus and sulfur can highly increase the corrosion rates in acids [15].

Therefore, the crevice maximum depth results for 416 type reviled higher results than 410 type, and that can be illustrated in Fig. 11. Another reason for the high corrosion rates of AISI 416 steel was that, corrosion rates increases with decreasing the spheroidization of carbides shapes, and that can be discussed later by the microstructure test and ImageJ results.

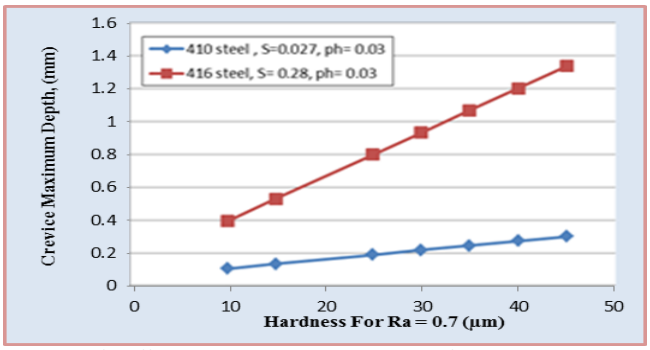

Fig. 11 Sulfur effects on the crevice corrosion rates for AISI 410 and 416

B.2. Surface Roughness Effects

Results showed that as surface roughness increased, the crevice maximum depth increased. It's seemed that for smooth surfaces, only few number of chloride ions were able to attack the surface at the crevice position, since valleys depths are small. Unlike rough surfaces, the depth of valleys inside crevice was more sufficient for chloride attacks to take place. The same behavior was reached by many researchers during their investigations for different corrosion and material types, but the difference was that each researcher attributed his results to different reasons.

On other side, the surface engineering handbook [16] indicates that during grinding process, residual stresses will take places on the ground specimen and located on the tip of the surface peaks, making the peaks good stress concentration regions for cracks to propagate. Generally, the presence of residual stresses during grinding was attributed to the action of both mechanical and thermal effects. During grinding the mechanical forces expand the specimen surface resulting with plastically deformed surface in a compressive residual stress condition. As the metal removal rate increases, the residual concentrations and the deformation increase. Another reason for the presence of residual stresses is the thermal effect during grinding. Increasing the temperature in the surface layer while the inner section remains cool, generated a deformed surface with a tensile residual stresses.

C. Microstructure Results

During the annealing processes (pretreatments) that were carried at 540˚C and followed by 790˚C, the refining of grains in the steels structure has no effect on their mechanical properties, because grain size has only effects on the ductile-brittle temperature transformation. Therefore, grain size refining of the ferritic structure (observed from microscopic results after annealing) has no effect on the decreasing of hardness results [11]. On other hand, the presence of chromium (strong carbide former) led to the formation of very small dispersed particles of chromium carbides which in turn results with decreasing the hardness values. For 416 steel, the carbide amounts are little higher than that for 410 steel and therefore the hardness is higher. Fig.12 illustrated the microscopic results for AISI 410 and 416 after pre-treating conditions.

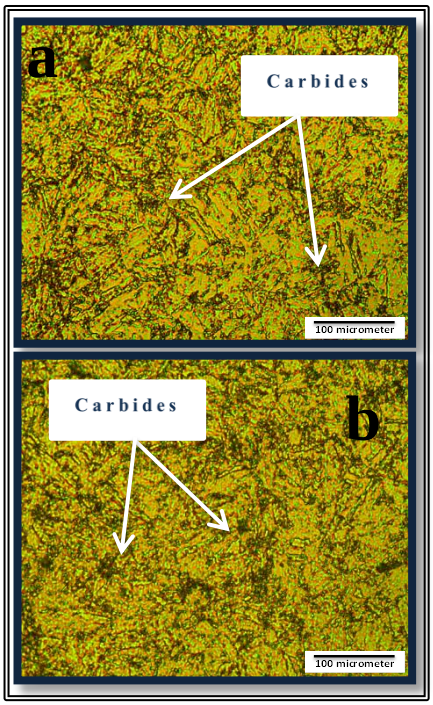

Fig. 12 Microstructure graph for a) AISI 410, annealed condition, 9.7 HRC, small limited particles of Cr carbides, fine ferritic grain sizes. b) AISI 416,annealed condition, 12.85 HRC, smaller limited of Cr carbides, fine ferritic grain sizes

After heating the metals to the austenitizing region, maximum hardness is achieved by quenching due to the formation of martensitic structure. Then, tempering process was used to reduce the high hardness values (resulted from the carbon that strained the iron lattice during quenching) by expelling the sub-cementite particles from the BCT lattice (body centered tetragonal) and forming the BCC lattice (body centered cubic). As tempering heating increases, the particles of carbides (cementite in addition to chromium carbides) grow by coalescence, and such increasing in the size of carbides will cause softening in the steel and decreases hardness [11]. Therefore due to the carbides coalescence process, the samples tempered with 565 or 605℃ contained larger and less amounts of carbides (Fig. 13, 14) so revealed lower hardness than samples tempered with 205, 230 or 370℃ that contain smaller and more carbide amounts (Fig. 15, 16).

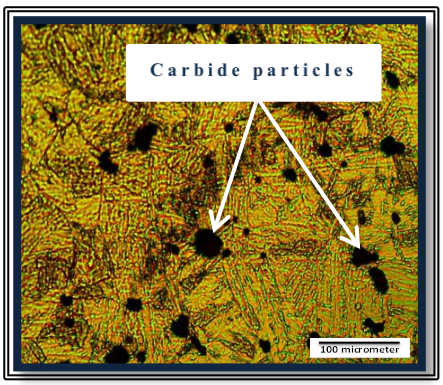

Fig. 13 Microstructure graphs for samples tempered with 605˚C, AISI 410, 24.45 HRC, larger particles of carbides, more spheroidization, coarse martensitic grain sizes

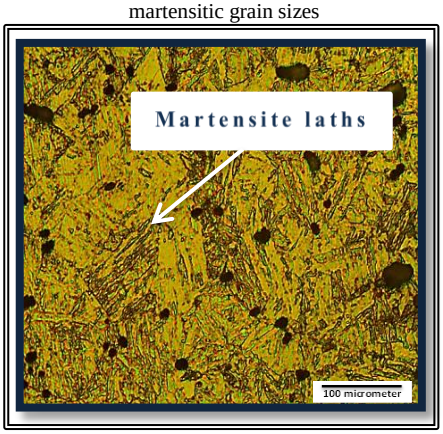

Fig. 14 Microstructure graphs for samples tempered with 605˚C, AISI 416 24.8 HRC, more particles of carbides, less spheroidization, coarse martensitic grain sizes

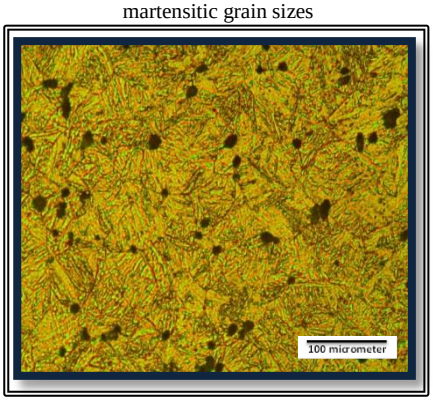

Fig. 15 Microstructure graphs for AISI 410 sample tempered with 370˚C, 39.7 HRC
Smaller carbides than Fig. 12(a)
More carbides than Fig. 12(a)

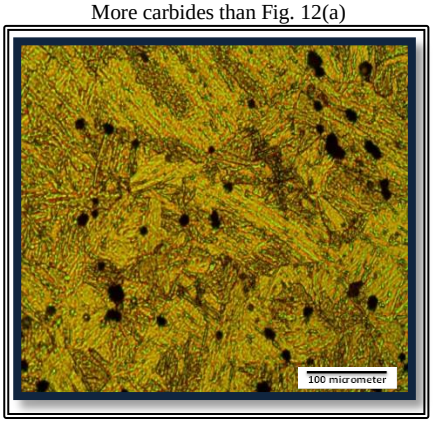

Fig. 16 Microstructure graphs for AISI 416 sample tempered with 370˚C, 38.7 HRC
Smaller carbides than Fig. 12 (b)
More carbides than Fig. 12 (b)

D. ImageJ Results

By using the ImageJ program, several micrographs obtained during microstructure test for AISI 410 steel samples of different hardness values were analyzed in order to determine the effects of carbides area on the hardness. By LAB-Fit program, the ImageJ results were used to predict the mathematical models (Eq. 3) for carbides average area (output) at different hardness results (inputs). The results proved that hardness increases by decreasing the average carbides area due to the coalescence behavior. Fig 17illustrated the predicted model of carbide average area for different hardness values.

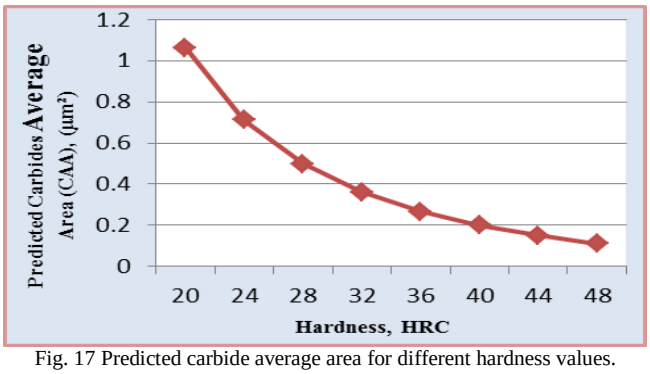

Fig. 17 Predicted carbide average area for different hardness values.

VI. Conclusion

Several important points were concluded from this study:

I-Crevice corrosion rate increases with increasing tempering hardness and surface roughness for both AISI 410 and 416 martensitic stainless steels.

II-Surface roughness effects on crevice maximum depth are higher than the effects of hardness.

III-AISI 416 steel revealed higher crevice corrosion rates than 410 steel, and that was due to the higher alloying element content and especially the higher sulfur content for 416 steels.

IV-Hardness increases with increasing the austenitizing temperature, but as the austenitizing temperature reached the higher limit (1000˚C) as the hardness begins to decrease. That was attributed to the chromium carbide precipitations that increased with increasing temperature, but for high temperature limit retained austenite begins to form causing the hardness values to be lowered.

V-For tempering temperatures above 400˚ C, hardness values were lower than that for tempering temperatures below 400℃. Such behavior was attributed to the carbides amount and carbides size. As tempering temperature increases, the carbides will grow up by coalescence causing the carbides size to be larger and the carbide amounts to be reduced so the hardness values to be decreased.

VII. REFRENCES

[1] Avesta Research Center, “Outokumpo Stainless AB Handbook”, Outokumpooyj, 2013.

[2] ASM International, “Heat Treating ASM Handbook”, Vol. 4, 1991.

[3]Thomas G. Digges Samuel J.Roseuberg, and Glenn W. Geil, “Heat Treatment and Proprties of Iron and Steel”, U. S. Government Printing Office, pp. 221-542, 1966.

[4] J. H. Dautzeuberg, and J. A. Kals, “Surface Roughness Caused by Metal Forming”, Annuals of the CIRP, Vol. 34, No. 1, 1985.

[5] J. E. Truman, "Corrosion Resistance of 13% Chromium Steels as Influenced by Tempering Treatments", Br. Corros. J. , Vol. 11, No. 2, 1976.
[6] R. Godec, and V. Dolecek, "Influence of Different Heat Treatments on Corrosion Resistance of Martensitic Stainless Steels", Werkstoffeand Korrosion, Vol. 45, pp. 517-522, 1994.
[7] G. I. Burstein, and P. C. Pistorius, "Surface Roughness and the Metastable Pitting of Stainless Steel in Chloride Solutions", Corrosion, Vol. 51, No. 5, 1995.
[8] G. T. Burstein, and S. P. Vines, "Repetitve Nucleation of Corrosion Pits on Stainless Steel and the Effects of Surface Roughness", Journal of the Electrochemical Society, Vol. 148, No. 12, B504-B516, 2001.
[9] T. Hong, and M. Nagumo, "Effect of Surface Roughness on Early Stages of Pitting Corrosion of Type 301 Stainless Steel", Corrosion Science, Vol. 39, No. 9, pp. 1665-1672, 1997.
[10] W. Li., and D. Y. Li., "Influence of Surface Morphology on Corrosion and Electronic Behavior", ActaMaterialia, Vol. 54, pp. 445-452, 2006.
[11] J. L. Smith, G. M. Russel, and S. C. Bhatia, "Heat Treatment of Metals", Stalish Kumar Jain for CBS Publishers and Distributors, 1st edition, ISBN:978-81-239-1644-6, Vol. 1, 2008.
[12]ASTM Designation G48-00, "Standard Tests Methods for Pitting and Crevice Resistance of Stainless Steels and Related Alloys by Use of Ferric Chloride Solution", Annual Book of ASTM Standard, Vol. 11-01.
[13]ASTM E3-01, "Standard Guide for Preparation of Metallographic Specimens", ASTM International, West Conshohocken, PA, 2007.
[14] ASTM E407-07, "Standard Practice for Microetching Metals and Alloys", ASTM International, 2015.
[15] R. Winston Revie, and Herbert H. Uhlig, "Corrosion and Corrosion Control", John Wiley and Sons, 4th edition, ISBN:978-0-471-73279-2, 2008.
[16] LAMET, and et. al, "Surface Engineering ASM Handbook", ASM International, ISBN: 0-87170-377-7, Vol. 5, 1994.

VIII. BIOGRAPHIES

Haider M. Mohammad HAS Ph.D. in Mechanical Engineering (Applied Mechanics, Failure of Materials) with University of Basrah, College of Engineering, Mechanical Eng. Dept. (with Research Scholarship at Cardiff School of Engineering – Wales – UK). He Interests with research areas of failure Boilers, corrosion, fatigue, creep rupture, surface roughness, heat treatment, welding, optimization, sustainability, cold working, and machining. He attained several conferences The 2nd International Conference for Mechanical Engineering, Technical College, Najaf, Iraq, Mar. 2013, International Conference for Mechanical and Material Engineering, University of Babylon , Iraq, May 2013, 11th Global Conference on Sustainable Manufacturing, Berlin, Germany, Sep. 2013, The 1st International Conference for Mechanical Engineering, College of Engineering, University of Basrah, Iraq, April 2014, The 1st Conference for Engineering, Technology, College of Engineering, University of Thi-Qar, Iraq, Oct. 2015 and the 7th Annual Congress on Materials Research and Technology, Feb. 2017.